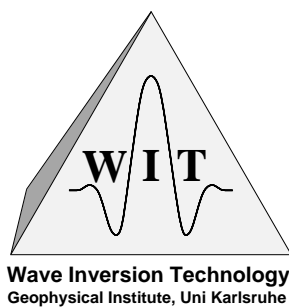


SEISMIC MODELING BY DEMIGRATION

*Lúcio T. Santos[†], Jörg Schleicher[†], Martin Tygel[†], and Peter Hubral**



Campinas, March 3, 1998

WIT Consortium Project

[†]: Dept. Applied Math., IMECC/UNICAMP, C.P. 6065, 13081-970 Campinas, SP,
Brazil

*: Geophysical Institute, Karlsruhe University, Hertzstr. 16, 76187 Karlsruhe,
Germany

GEOPHYSICS, **65**, no. 4, 1281–1289 (2000)

presented at the 67th SEG Meeting, Dallas, TX

ABSTRACT

Kirchhoff-type, isochrone-stack demigration is the natural asymptotic inverse to classical Kirchhoff or diffraction-stack migration. Both stacking operations can be performed in true amplitude by an appropriate selection of weight functions. Isochrone-stack demigration can be also used for seismic modeling purposes, i.e., for the computation of synthetic seismograms. The idea is to attach to each reflector in the model an appropriately stretched (i.e., frequency shifted) spatial wavelet with an amplitude proportional to the reflection coefficient, so that the reflector model is transformed into an artificially constructed true-amplitude depth-migrated section. The seismic modeling is then realized by a true-amplitude demigration operation applied to this artificial migrated section. Two simple but typical synthetic data examples indicate that modeling by demigration yields superior results as compared to conventional zero-order ray theory or even classical Kirchhoff modeling. Modeling by demigration turns out to be particularly advantageous when repeated seismic modeling, as in time-lapse seismic reservoir modeling, or modeling for nonsmooth reflectors is required. Moreover, modeling by demigration links the theory of seismic modeling to that of seismic reflection imaging. Any software developed for true-amplitude Kirchhoff migration can be easily modified to construct synthetic seismograms with the help of true-amplitude modeling by demigration.

INTRODUCTION

True-amplitude Kirchhoff-type depth migration is a most desirable seismic imaging tool. It transforms a given time section into a depth-migrated section, in which the migrated seismic pulses along the reflectors are free from geometrical-spreading losses (see, e.g., Bleistein, 1987; Schleicher et al., 1993; Sun and Gajewski, 1997). Neglecting all other factors that affect amplitudes as, e.g., transmission and attenuation losses (for other amplitude factors see Sheriff, 1975) and ignoring multiple arrivals present in the original seismic time section, the true-amplitude depth migration output at each point of a reflector is a measure of the reflection coefficient. This coefficient pertains to the primary-reflection ray joining the source to the receiver position in the given measurement configuration. The considered point on the reflector is the specular reflection point of this ray.

Each reflector in the depth-migrated section appears as a certain strip of spatial wavelets of varying width. The form of this spatial wavelet strip is determined by the input temporal pulse

(i.e., the source pulse), as well as by the so-called stretch factor. The latter describes the distortion, also called the frequency shift, of the pulse due to the migration process (Brown, 1994; Tygel et al., 1994b).

The diffraction-stack or Kirchhoff migration integral is often understood, in an asymptotic sense, as the inverse operation to forward modeling with the classical Kirchhoff integral (Frazer and Sen, 1985). As it is well known, the Kirchhoff integral can be used to propagate a given incident wavefield (e.g., an elementary compressional wave) from the reflector to the receiver point by superposing “Huygens’ secondary sources.” In the same way, the Kirchhoff migration integral serves to reconstruct the same Huygens’ secondary sources along the reflector (in position and strength) from the measured elementary-wavefield reflections at several receiver positions along the seismic line. Note, however, that the Kirchhoff migration integral only inverts the propagation effects of the Kirchhoff integral (Tygel et al., 1994a). To reconstruct the physical model, an additional process (usually called inversion) is needed.

As discussed by Hubral et al. (1996) and mathematically shown by Tygel et al. (1996), there exists another inverse to the Kirchhoff migration integral (also in an asymptotic sense). This inverse has the same integral structure as Kirchhoff migration. It is given by an stacking process which is applied to the depth-migrated section. To better understand the process, we first recall that the Kirchhoff depth-migrated section is constructed by stacking the original seismic time-domain data along certain stacking surfaces (or lines in two dimensions). These are constructed on a given macrovelocity model without the need to determine (nor to identify) the location of the reflection traveltime surfaces in the seismic section. The inverse process can be formulated by a similar stack along related surfaces. These are also constructed on the given macrovelocity model without knowing the location of the reflectors in the migrated section. The stacking surfaces are simply the isochrones, i.e, the surfaces of equal reflection time between a given source and receiver. These isochrones (ellipsoids in the constant-velocity case) are defined by the same traveltimes as the Kirchhoff-type diffraction traveltime surfaces (hyperboloids in the constant-velocity case) that define the stacking surfaces for migration. Thus, all that is to be known to actually perform the inverse stacking-based reflection imaging process is the same macrovelocity model as previously used for the Kirchhoff migration. Because of its fundamental similarity to Kirchhoff migration, the can be called an isochrone stack or simply *Kirchhoff demigration*.

Although being a very recent development, seismic demigration is, however, not a process unknown to the seismic world (Whitcombe, 1991; Kaculini, 1994). It has already found several different types of practical applications.

One of the first seismic methods to be suggested that are based on the cascaded application of migration and demigration is the so-called “seismic migration aided reflection tomography” or briefly SMART (Faye and Jeannot, 1986; Lailly and Sinoquet, 1996). Here, seismic reflection data are migrated to depth using a simple, albeit probably wrong, macrovelocity model. In the depth domain, the migrated primary reflection events, although erroneous, are usually more coherent and can, thus, be better identified and picked. The resulting picked “reflector maps” are then kinematically demigrated back into the time domain using the same macrovelocity model. The demigrated reflector images can then help to identify and pick the traveltimes surfaces in the original seismic data. A similar concept was independently described by Fagin (1994).

The same cascade of migration and demigration is also used in a non-layer-stripping approach for depth-conversion purposes. As described by Whitcombe (1991; 1994), the combination of demigration with single-step ray migration can be used to fastly improve a layered macrovelocity model. In this procedure, demigration is used to back out the effect of time migration prior to a ray-based depth migration (i.e., map migration) and to enable the lateral shift between the time migrated image and a depth-migrated image. The needed velocity model is obtained from a conventional vertical depth conversion of time-migrated data.

Another important field, where demigration has already found a practical application is velocity analysis (Ferber, 1994). The procedure is similar to a conventional migration velocity analysis. Conventionally, image gathers are formed after prestack depth migration in the migrated domain. Of course, all so-obtained migrated seismic image gathers to be compared depend on the macrovelocity model, which will be generally incorrect. Thus, an interpretation of the image gathers may be difficult. Demigration can be used to avoid this problem by enabling a comparison directly between seismic time sections. All that has to be done is to demigrate the migrated sections obtained from different common-offset sections using the original macrovelocity model. However, instead of demigrating them back to their original offset, demigration is applied to all of them using a given, fixed offset that was actually used in the data acquisition geometry. After demigration, all so-obtained sections can be compared with a real common-offset section that was actually measured in the field. The advantage is that the latter obviously does not depend on the macrovelocity

model. Of course, if the macrovelocity model was correct, all constructed offset sections should be identical to each other and to the section actually measured. Deviations between the constructed and measured sections can therefore be directly attributed to errors in the macrovelocity model. These deviations can be determined, interpreted, and used to update the velocity model in the same way as in migration velocity analysis.

Moreover, the processing sequence of migration and demigration has the potential of being utilized in data regularization. Seismic reflection data that were acquired on an irregular grid can be migrated to depth (using a macrovelocity model as accurate as possible) and then demigrated with the same model back into the time-domain data space onto a regular grid. Although expensive, this is the best data interpolation (and even extrapolation) technique as it correctly accounts for the propagation effects in the reflector overburden.

The fact that the familiar Kirchhoff migration integral seems to have “two inverse integrals” (in an asymptotic sense) leads inevitably to the question whether the two processes described by these integrals are identical. The answer is that these are, although closely related, in fact different processes. Their close relationship, however, implies the conclusion that it should be possible to use Kirchhoff demigration to achieve the goals of the forward Kirchhoff modeling. In this paper, we elaborate on how this can be done.

Although the two integrals describing Kirchhoff forward modeling and Kirchhoff demigration both appear to be inverses to Kirchhoff migration in an asymptotic sense, they do not exactly coincide. Their relationship was recently investigated by Jaramillo and Bleistein (1997). Considering only the leading order contributions, they have shown that the Kirchhoff modeling integral can be modified in such a way that the Kirchhoff demigration integral results. As the main contributions to the integration stem from the specular reflection point, this modification should not cause major differences. We may, thus, interpret the demigration integral as a “reorganized Kirchhoff modeling integral,” which should give similar if not identical results. The physical interpretation of this new integral is, however, different. Unlike the Huygens’ secondary source contributions in the Kirchhoff integral, it is now the individual Fresnel zone contributions to each primary reflection that are summed up by the integration (Schleicher et al., 1997).

What are, then, the advantages of implementing a seismic modeling scheme using the Kirchhoff demigration integral instead of the conventional Kirchhoff modeling integral? Well, in fact,

there exist several reasons:

- The actual process of true-amplitude Kirchhoff demigration is so similar to true-amplitude Kirchhoff migration that existing migration programs (which are nowadays, of course, highly developed and very effective) can be readily modified to include the demigration and also the seismic modeling part.
- Demigration is a process that becomes more and more important in the seismic processing sequence in the pursuit to verify and improve the macrovelocity model. In this way, seismic modeling can be done with a software that is also useful for reflection-imaging purposes and thus already available. No additional seismic forward modeling program is necessary.
- The Green's functions needed for migration and demigration are actually the same. So, when applying demigration (either for seismic modeling or imaging purposes), using a velocity model for which some time-domain data have been previously migrated, the Green's functions are already available thus turning the demigration less expensive.
- Modeling by demigration turns out to be a particularly advantageous process when the effects of reservoir changes are to be modeled as is the case in 4-D or time-lapse imaging. As only the reflector properties change but not the overburden with its propagation effects, the same Green's functions can be used several times for subsequent modeling thus making modeling by demigration superior in comparison with other schemes that have to start all over again.
- As demigration is a stacking process, it "smoothes" the simulated reflection responses (in contrary to, e.g., standard ray theory that computes arrival times and amplitudes along specular rays only). Thus, there is no need for constructing smooth reflectors (e.g., by applying splines) or explicit two-point ray tracing. Modeling by demigration can be directly applied to the conventionally picked reflectors that are usually a sequence of planar reflector elements. This will not cause any damage to the simulated reflection response.
- Whereas Kirchhoff modeling needs an integration along the reflector and, thus, has to be applied to each reflector independently, demigration uses as its input a depth-migrated section. It thus needs to be applied only once to model primary reflections for a whole set of different subsurface reflectors.

- Because the demigration integral sums only contributions from the actual Fresnel zone surrounding each specular reflection point, the stacking aperture can be even further reduced.

However, it should be kept in mind that Kirchhoff demigration is a process as expensive as Kirchhoff migration. It may, thus, be disadvantageous in comparison to other seismic modeling schemes, particularly when applied only once for a given velocity model, for a few reflectors only, or for the purpose of including multiples, etc.

MODELING, MIGRATION, AND DEMIGRATION

Before introducing seismic modeling by demigration as a tool for the construction of synthetic seismograms, let us firstly comment on the basic characteristics of the two processes of modeling and demigration themselves, so as to appreciate their similarities and differences.

Basic model assumptions

Throughout this paper, we assume that primary elementary wave propagation is to be modeled in a layered, isotropic, inhomogeneous earth model with smoothly curved interfaces (see Figure 1). Within the layers, the medium parameters vary smoothly such that a high-frequency approximation is justified.

To better explain the principles underlying modeling by demigration, we arbitrarily choose one of the many reflecting interfaces as the target reflector. Of course, the process described below for one reflector and its primary elementary reflection simultaneously applies to all interfaces for which elementary primary reflection responses are to be modeled.

For reasons of simplicity, we refrain from including transmission losses within the overburden of the chosen target reflector into the following discussions. However, please keep in mind that all overburden effects can be appropriately accounted for by including them into the necessary Green's functions computations. This is true for Kirchhoff modeling as well as for Kirchhoff migration and demigration.

Modeling versus demigration

Modeling, as we understand it, implies the analytical or numerical simulation of a physical process given all the equations and parameters for its complete description. In our case, the physical process to be simulated is seismic wave propagation. It is described, e.g., by the elastic or acoustic wave equation and the parameters are the velocity and density distributions within the medium, the source and receiver locations, and the source wavelet together with appropriate boundary and initial conditions. Seismic modeling is, then, realized by an implementation of the wave equation (e.g., using finite differences or the Born or Kirchhoff representation integrals) or its approximate solutions (like asymptotic ray theory) to obtain a synthetic-seismogram equivalent of the seismic data that would have been recorded if the same experiment had been actually carried out in the field. For the meaningful case of a layered Earth model, we need, in particular, the precise location and description of the interfaces, as well as the appropriate boundary conditions on them.

Demigration, on the other hand, although it envisages to provide very similar results, uses a conceptually different approach. Its aim is to reconstruct a seismic time section from a corresponding depth-migrated section. In other words, demigration aims to invert the imaging process of migration. Of course, as migration aims at inverting the wave propagation effects, it is related in some way to the wave equation. Correspondingly, also demigration, as the inverse process to migration, must have some relationship to that equation. As opposed to direct forward modeling, however, we do not have to implement or even know this wave equation. Moreover, we do not have to precisely know all the true model parameters to actually perform the demigration process. Neither the true velocity distribution in the earth, nor the source wavelet nor, above all, the position of the reflecting interfaces have to be known in order to apply a demigration. All that is needed, apart from the seismic depth-migrated image section to be demigrated, is the macrovelocity model that has been used for the migration process which produced this section. In fact, a table with all the Green's functions as used in migration (i.e., from all sources and receivers to all subsurface points on an appropriate grid) would already be sufficient. Of course, the better the macrovelocity model is, the better will be the corresponding migrated section. This is, however, a problem of migration and not of demigration. Even if the velocity model used for the original migration was very poor and thus the depth-migrated image of very bad quality, a subsequent demigration will correctly reconstruct the original time section. The only condition is that the same macrovelocity model has to be used for demigration as previously used for migration. In other words, the chain of migration

and demigration is a process that recovers the original time-domain data (in a high-frequency sense) with very little sensitivity to the macrovelocity model.

After having qualitatively clarified the terms modeling and demigration, let us now mathematically describe them in order to better understand their relationship.

Modeling

For reasons of comparison, we choose the well-known Kirchhoff integral to represent a seismic forward modeling scheme. It can be written as (Frazer and Sen, 1985; Tygel et al., 1994a)

$$\mathcal{K}(\xi, t) = \frac{1}{2\pi} \iint_{\Sigma} dS W(\xi, P_{\Sigma}) \partial_t F[t - \tau(\xi, P_{\Sigma})], \quad (1)$$

where $\mathcal{K}(\xi, t)$ denotes the modeled synthetic seismogram and $z = \Sigma(x)$ is the reflector along which we have to integrate. We remind that for many reflectors, an integral of this type has to be solved along each of them. Also, $W(\xi, P_{\Sigma})$ is a kernel or weight function consisting of an obliquity factor, the specular plane-wave reflection coefficient $\mathcal{R}(P_{\Sigma})$ of the incident wave at the reflector, and two Green's function amplitudes. The latter pertain to the wave propagation along the two paths from the source $S(\xi)$ to the point $P_{\Sigma} = (x, z = \Sigma(x))$ on the reflector, and from there to the receiver $G(\xi)$ (see Figure 1). Here, ξ denotes a parameter that describes the measurement configuration. Moreover, $F[t]$ is the analytic pulse that is chosen to represent the source signature and

$$\tau(\xi, P_{\Sigma}) = T(S(\xi), P_{\Sigma}) + T(G(\xi), P_{\Sigma}) \quad (2)$$

is the sum of traveltimes along the two paths of propagation SP_{Σ} and GP_{Σ} , where $S(\xi)$ and $G(\xi)$ are fixed and P_{Σ} varies along the reflector.

The subsequent discussion is by no means restricted to a certain number of dimensions. We choose to discuss the situation in three dimensions with x and ξ being 2-D vectors representing the two horizontal coordinates. However, those readers who prefer to think in two dimensions need only to think of x and ξ as scalars in the in-line direction and all integrals as being line integrals instead of surface integrals.

As it is well-known, the integral (1) can be asymptotically evaluated as the sum of contributions of its stationary points. To leading order, these are the specular reflection points $P_R(\xi) = P_{\Sigma}|_{x^*(\xi)}$ on the reflector that pertain to the given source-receiver pair $S(\xi)$ and $G(\xi)$

specified by ξ . Assuming, for simplicity, a unique specular reflection P_R (see Figure 1), the asymptotic evaluation yields the zero-order ray approximation

$$\mathbb{K}(\xi, t) \approx \frac{\mathcal{R}(\xi)}{\mathcal{L}(\xi)} F[t - \mathcal{T}(\xi)] , \quad (3)$$

where $\mathcal{R}(\xi) = \mathcal{R}(P_R)$ is the reflection coefficient, $\mathcal{L}(\xi)$ is the geometrical-spreading factor, and $\mathcal{T}(\xi) = \tau(\xi, P_R)$ is the reflection traveltime. All of these quantities pertain to the specular ray SP_RG . Of course, for many reflectors, the modeled synthetic seismogram section will be a superposition of elementary primary reflections of type (3).

We stress again that here as well as in the following, additional amplitude effects as, e.g., due to transmission losses at overburden interfaces, absorption, etc, are, for simplicity, neglected. These effects can be included independently into each of the methods to be discussed in this paper.

Migration

Kirchhoff migration is based on the idea of stacking the time-domain data in such a way that any reflection possibly pertaining to a certain, arbitrarily chosen depth point $P = (x, z)$ is summed up. Kirchhoff migration can be represented by the following stacking integral (Bleistein, 1987; Schleicher et al., 1993)

$$\mathbb{M}(x, z) = -\frac{1}{2\pi} \iint_A d^2\xi W_M(\xi, P) \partial_t D(\xi, t)|_{t=\tau(\xi, P)} , \quad (4)$$

where $\mathbb{M}(x, z)$ denotes the depth-migrated data, $W_M(\xi, P)$ is the true-amplitude weight function that guarantees a correct amplitude treatment, and $D(\xi, t)$ are the seismic time-domain data to be migrated. Also, A is the migration aperture. In correspondence to equation (2),

$$\tau(\xi, P) = T(S(\xi), P) + T(G(\xi), P) \quad (5)$$

is the sum of traveltimes along the two paths of propagation SP and PG , where now, however, P is an arbitrary, fixed point in the subsurface and $S(\xi)$ and $G(\xi)$ vary along the measurement surface (see again Figure 1).

Correspondingly to the above, also integral (4) can be evaluated asymptotically. For all primary reflections described in zero-order ray theoretical approximation according to equation (3), an evaluation of the Kirchhoff migration integral (4) in the vicinity of a specular reflection

point P_R on an actual reflector $z = \Sigma(x)$ (see Figure 1) yields the reflector image (Tygel et al., 1996)

$$M(x, z) \approx \mathcal{R}(\xi^*) F[\mathcal{S}(x)(z - \Sigma(x))]. \quad (6)$$

In other words, Kirchhoff migration (4) reconstructs the source wavelet in the vicinity of point P_R on the reflector $z = \Sigma(x)$. The point P_R determines the stationary point ξ^* of integral (4) which, in turn, defines the specularly reflected ray $S(\xi^*)P_R G(\xi^*)$. The peak amplitude of the migrated pulse is given by the reflection coefficient $\mathcal{R}(\xi^*)$. Thus, Kirchhoff migration (4) frees the primary reflection event $D(\xi^*, t)$ from its geometrical-spreading loss, however stretching the wavelet by the factor (Tygel et al., 1994b)

$$\mathcal{S}(x) = \frac{2 \cos \alpha_R \cos \beta_R}{v_R}, \quad (7)$$

where α_R is the reflection angle, β_R is the local (in-plane) reflector dip angle, and v_R is the velocity at the specular reflection point P_R . Further away from the reflector, the stack (4) yields a negligible value.

The main advantage of Kirchhoff migration (4) is that neither the primary reflections nor the reflector positions need to be identified. The same integration (or stacking) process is applied, independently of the number and location of the primary reflection events and reflecting interfaces. All reflector images will be represented by an expression of type (6).

Note that although often referred to as such, migration is not a complete inverse process to modeling, not even in an approximate sense. Migration does not reconstruct the original Earth model with all its physical parameters that are needed as the input to forward modeling. This is done by an additional process called inversion. It is usually applied in a chain with migration which is then referred to as migration/inversion. Without the inversion step, a migrated section cannot be used as an input to modeling. It can, however, be used directly as an input to demigration.

Demigration

From corresponding arguments as for Kirchhoff migration, a structurally equivalent integral can be set up for its inverse operation (Hubral et al., 1996; Tygel et al., 1996). The idea is to stack along a certain surface in the depth-migrated data volume in such a way that any migrated event that possibly pertains to a certain, fixed data point $N = (\xi, t)$ in the unmigrated section is summed

up. This process is represented by the Kirchhoff demigration integral

$$\mathcal{ID}(\xi, t) = \frac{1}{2\pi} \iint_E d^2x W_D(x, \xi, t) \partial_z M(x, z)|_{z=\zeta(x, \xi, t)}, \quad (8)$$

where $\mathcal{ID}(\xi, t)$ denotes the *demigrated data*, $W_D(x, \xi, t)$ is again a true-amplitude weight function to treat amplitudes correctly, and $M(x, z)$ is the migrated image obtained from a previous migration, although not necessarily from a Kirchhoff migration. Moreover, E is the spatial aperture of demigration. The stacking surface, $z = \zeta(x, \xi, t)$, is implicitly given by

$$t = \tau(\xi, x, z = \zeta(x, \xi, t)) = T(S(\xi), P) + T(G(\xi), P), \quad (9)$$

i.e., again by the very same sum of traveltimes (2) as used in Kirchhoff forward modeling (1) and Kirchhoff migration (4). As in Kirchhoff modeling, $S(\xi)$ and $G(\xi)$ are the fixed source and receiver points. Other than in that case, however, $P = (x, z)$ does not vary along the reflector $z = \Sigma(x)$ but along the surface $z = \zeta(x, \xi, t)$ that defined by equation (9) under the condition that t is constant. In other words, $z = \zeta(x, \xi, t)$ describes the surface of equal reflection time or *isochrone* pertaining to the fixed source-receiver pair S and G and a given time t (see again Figure 1). This isochrone plays the same role in Kirchhoff demigration (8) as the diffraction-time surface plays in Kirchhoff migration (4). In both cases, the stacks sum up all contributions that come from the Fresnel zones surrounding the specular reflection points.

Let us assume that the original time-domain data were migrated using some migration scheme of which the amplitude and stretching properties are unknown. Then, the resulting reflector images can still be represented, correspondingly to equation (6), by an expression of the type

$$M(x, z) = \mathcal{A}(x)F[\mathcal{P}(x)(z - \Sigma(x))], \quad (10)$$

where \mathcal{A} describes the amplitude of the migrated reflections and \mathcal{P} is a certain “prestretch factor” produced by the migration operation. Application of the above demigration integral (8) to the reflector image (10) yields, after asymptotic evaluation as before,

$$\mathcal{ID}(\xi, t) \approx \frac{\mathcal{A}(x^*)}{\mathcal{L}(\xi)} F[S(x^*)^{-1} \mathcal{P}(x^*)(t - \mathcal{T}(\xi))], \quad (11)$$

where $x^* = x^*(\xi)$ is the stationary point describing the specular reflection ray $S(\xi)P_R G(\xi)$. Note that the amplitude after true-amplitude demigration becomes a fraction in which the numerator $\mathcal{A}(x^*)$ is the original amplitude of the input migrated section evaluated at the stationary point. The denominator is the geometrical-spreading factor $\mathcal{L}(\xi)$ along the reflection ray $S(\xi)P_R G(\xi)$. This is

to be contrasted with true-amplitude migration where the geometrical-spreading factor has been removed from the input amplitudes [see equation (6)].

It was shown by Tygel et al. (1995) that the pulse stretch caused by demigration is the inverse to that introduced by migration. It is given by equation (7). In other words, Kirchhoff demigration “unstretches” the seismic signal by the same factor \mathcal{S} by which Kirchhoff migration stretches it. Hence, after Kirchhoff migration and demigration, no overall stretch factor remains in formula (11).

Like Kirchhoff migration, also Kirchhoff demigration does not depend on the number and locations of primary reflections or reflector images. The demigrated section will thus be a superposition of all demigrated reflector images (i.e., primary reflection events) of the type of equation (11).

Asymptotic inverses

If we apply Kirchhoff forward modeling (1) to a certain model containing a target reflector $z = \Sigma(x)$, and, afterwards, Kirchhoff migration (4) to the resulting synthetic reflection data $\mathcal{IK}(\xi, t)$ using the same velocity model for both operations, then the migration result $\mathcal{IM}(x, z)$ will approximate the reflector image (6). Ideally, we would like to have Kirchhoff migration (4) reconstruct the original model, i.e., we would like migration to be an (asymptotic) inverse to forward modeling. However, this is not the case. To actually reconstruct the physical model, we need to add another process, inversion, to extract the model parameters and the reflector locations from the migrated sections. We may then say that only the combined process of migration/inversion is a complete (asymptotic) inverse to modeling.

On the other hand, we may apply Kirchhoff migration (4) to some given field data $D(\xi, t)$, and then Kirchhoff demigration (8) to the resulting migrated section $\mathcal{IM}(x, z)$, using the same macrovelocity model in both operations. Then, the demigration result $\mathcal{ID}(x, t)$ can be expected to closely reconstruct the original field data: $\mathcal{ID}(\xi, t) \approx D(\xi, t)$. Thus, Kirchhoff demigration (8) can be conceived as an (asymptotic) inverse to Kirchhoff migration (4).

From the above observations and speaking in an asymptotic sense, we conclude that Kirchhoff modeling and demigration are two processes that are closely related but not identical. Whereas Kirchhoff demigration is the inverse process to Kirchhoff migration, Kirchhoff modeling is the

inverse operation to Kirchhoff migration/inversion. Nevertheless, the Kirchhoff demigration integral (8) can be employed for modeling purposes. In order to use Kirchhoff demigration in a process equivalent to Kirchhoff modeling, we obviously have to add another process, which has to be the “inverse operation to inversion.” How this can be done is investigated in detail in the next section.

Even apart from the mentioned inverse operation to inversion, the integrals (1) and (8) are not identical but account for the wavefield contributions to a specular reflection in a different way. Motivated by the work of Tygel et al. (1996), Jaramillo and Bleistein (1997) have shown that the Kirchhoff modeling and demigration integrals (1) and (8) are asymptotically (i.e., considering the leading order contributions only) equivalent to each other.

MODELING USING DEMIGRATION

After having stated the similarities and differences of modeling and demigration, let us address the basic question of this paper: How can we make use of the demigration for seismic modeling purposes? Well, for each given subsurface reflector, we have to appropriately *simulate* its corresponding true-amplitude depth-migrated reflector image *as if* obtained from a Kirchhoff migration applied to the primary reflection to be modeled. In other words, given the source and receiver positions, $S(\xi)$ and $G(\xi)$, respectively, as well as the reflector $z = \Sigma(x)$ within the velocity model and the analytic source signal $F[t]$, we have to artificially *construct* the true-amplitude reflector image

$$M(x, z) = \mathcal{A}(x)F[\mathcal{P}(x)(z - \Sigma(x))] . \quad (12)$$

This is obtained by placing the correctly scaled and stretched source pulse $F[t]$ along the reflector. Here, the amplitude factor $\mathcal{A}(x)$ and the prestretch factor $\mathcal{P}(x)$ have yet to be chosen in such a way that at the stationary point, $x^* = x^*(\xi)$, they equal the correct (plane-wave) reflection coefficient $\mathcal{R}(\xi)$ and the correct pulse stretch factor $\mathcal{S}(x^*(\xi))$, respectively, viz.

$$\mathcal{A}(x^*) \approx \mathcal{R}(\xi) \quad (13)$$

and

$$\mathcal{P}(x^*) \approx \mathcal{S}(x^*) . \quad (14)$$

This construction of an artificial migrated section is, in fact, the process that was referred to above as the “inverse operation to inversion.”

A natural choice for \mathcal{A} and \mathcal{P} is to use the actual functions \mathcal{R} and \mathcal{S} of Kirchhoff migration. Unfortunately, this might be difficult as these functions are correctly known only after the specular reflection rays are determined. Note, however, that any other pair of smooth functions \mathcal{A} and \mathcal{P} that satisfy conditions (13) and (14) at the stationary point will also work. This is an important observation as, for each reflector point, it allows to directly use the stationary value of the two functions without the need to compute them for other, more distant points.

Application of the demigration integral (8) to an artificial migrated section containing a superposition of reflector images of the type (12) with amplitude \mathcal{A} and prestretch factor \mathcal{P} such that, at the stationary point, they satisfy equations (13) and (14), respectively, leads, correspondingly to equation (11), to a “demigrated” or synthetic seismogram section where all specular primary reflections are of the type

$$ID(\xi, t) \approx \frac{\mathcal{R}(\xi)}{\mathcal{L}(\xi)} F[t - \mathcal{T}(\xi)] . \quad (15)$$

A comparison to equation (3) shows that this is exactly the result of zero-order ray theory or of the high-frequency evaluation of the Kirchhoff modeling integral (1). In other words, for specular reflections the synthetic time section obtained by demigration of this *artificially constructed* depth-migrated section will then be equivalent to the one directly obtained as a result of conventional elementary primary-wave forward modeling applied to the given subsurface reflectors. In addition to the correctly modeled specular reflections (15), modeling by demigration turns out to also provide good estimates of nonspecular events like diffractions or the wavefield near a caustic, as we will see below in the numerical examples.

The construction of the artificial migrated section has, in principle, to be done with the very same parameters that are needed for forward modeling. Of course, it is a natural choice to assume the true velocity distribution for this purpose. However, it is important to note that this is not the only possibility. We have already noted above that the sequence of migration and demigration is rather insensitive to changes in the velocity model. This has the following important consequence. When forward modeling by demigration is applied to a reflector model derived from a depth migration, the quality of that model is not very crucial in order to get synthetic seismograms that represent the observed field data very well. This implies, of course, that a good agreement of the synthetic seismograms with the observed field data does not necessarily mean that the involved macrovelocity model is a good one.

Implementational aspects

Kirchhoff demigration is a process that is completely parallel to Kirchhoff migration. Accordingly, it is implemented efficiently in the same way as the latter. Tables of Green’s functions from all source and receiver points to all subsurface points within a target region have to be computed. These provide not only the information about the isochrone stacking surfaces but also about the necessary weight functions along them. However, modeling by demigration includes an additional step, namely the construction of the true-amplitude reflector images in an artificial migrated section. This process was called above the “inverse operation to inversion.” In this section, we comment on how this part of the modeling process can be realized.

We have already observed that the stationary values (i.e., those pertaining to the specular ray) of the reflection coefficient \mathcal{R} and of the stretch factor \mathcal{S} are needed for the construction of the artificial migrated section. These are, of course, unknown before the specular ray is available. Although this seems to be a problem that can be solved by a preceding explicit two-point ray tracing only, it can, in fact, be circumvented.

Zero offset.—For zero-offset modeling, the above-explained idea of modeling by demigration can be directly applied. All necessary quantities to construct the migrated image for each reflector are physical parameters directly available from the a-priori specified Earth model. For any arbitrary zero-offset reflection, the stretch factor at the stationary point on the reflector is given by (Tygel et al., 1994b)

$$\mathcal{S} = \frac{2 \cos \beta}{v_1} \quad (16)$$

and the normal-incidence reflection coefficient by

$$\mathcal{R} = \frac{\rho_1 v_2 - \rho_2 v_1}{\rho_1 v_2 + \rho_2 v_1} \quad (17)$$

where β is the local reflector dip, and $v_{1,2}$ and $\rho_{1,2}$ are the velocities and densities above and below the considered target reflector at the reflection point. Therefore, \mathcal{S} and \mathcal{R} can be directly computed for any given reflector point. As all quantities are readily available from the specified Earth model, the construction of the artificial migrated section with true-amplitude reflector images of type (12) presents no problem.

Finite offset.—For nonzero offsets, modeling by demigration is a little more difficult. Before being attached to the reflectors in order to construct the artificial migrated section, the wavelet has to be multiplied by an amplitude factor \mathcal{A} that satisfies equation (13). It also needs to be stretched by a factor \mathcal{P} that satisfies equation (14). We recall that demigration will then “unstretch” the spatial wavelets of the reflector image (12), because it is the inverse process to migration. Therefore, the primary-reflection pulses (15) in the resulting synthetic-seismogram section become correct and do not suffer from any stretch.

In this case, the computational problem with equations (13) and (14) is that the stretch factor as well as the reflection coefficient at the specular reflection point depend on the reflection angle α_R of the specular reflected ray between $S(\xi)$ and $G(\xi)$ (see again Figure 1). This means, of course, that for each different source-receiver pair in the considered measurement configuration, a differently scaled and stretched wavelet is to be used because the reflection angle differs. As this angle is not available without previously determining the reflection ray between $S(\xi)$ and $G(\xi)$, a two-point ray tracing is, in principle, necessary to construct the artificial migrated section.

Below we will show that the artificial migrated section need not be constructed explicitly but only implicitly *during* the demigration procedure. Thus, the reflection angle α_R need not be known a priori, which means that a preceding two-point ray tracing is not necessary. This is, of course, important for reasons of efficiency. If one wanted to construct the artificial migrated section explicitly (as it has been done in this paper for didactical reasons), one would have to determine firstly the correct angle-dependent plane-wave reflection coefficient and the stretch factor (7) for each reflection point P_R on the reflector (see Figure 1). As in the zero-offset case, one would need the local in-plane dip angle β_R of the reflector and the velocities and densities above and below each considered reflector point. Moreover one would also need to know the true specular reflection angle α_R for the considered source-receiver pair $S(\xi), G(\xi)$ at each reflector point P_R . This knowledge could be obtained by two-point ray tracing from all sources $S(\xi)$ to all receivers $G(\xi)$. This would be an expensive process, even though it can be realized by searching the already computed Green’s functions tables for specular reflected rays. In this way, the artificial migrated section would be, in fact, constructed explicitly *before* the actual demigration is carried out. This is, however, a manner of solving the problem that is useful for didactical reasons only. It is very easy to do this for a constant-velocity medium, where the specular quantities can be directly computed using analytic expressions. In inhomogeneous media however, it would be too tedious and expensive to explicitly

construct the reflector images in the artificial migrated section.

For practical implementations, there exists a way of economizing on modeling by demigration. It is possible to use the information about the location and form of the true-amplitude target reflector image only implicitly. In this way, the amplitude and stretch factors are computed correctly *during* the modeling-by-demigration process. The artificial migrated section is actually never constructed explicitly. Its construction is realized only implicitly by the use of the reflector location and the source wavelet during the stack at each point on the isochrone.

The basic observation is that for each primary reflection to be modeled, equations (13) and (14) have to be satisfied only at the stationary point, i.e., at the specular reflection point P_R in Figure 1. Thus, the specular reflection angle α_R , which is the crucial and problematic quantity in the process, can be replaced at each “potential reflection point P ” on the isochrone by the half-angle α between the ray branches from the source $S(\xi)$ and the receiver $G(\xi)$ to this point. If a certain depth point on the isochrone is an actual specular reflection point P_R for the considered source-receiver pair $S(\xi), G(\xi)$, then this half-angle is equal to the specular reflection angle α_R . Therefore, conditions (13) and (14) are satisfied. Of course, the contributions from other reflector points that are not specular reflection points for the considered source-receiver pair are altered by this substitution. However, to the leading asymptotic order, the resulting alterations in the stacking sum are negligible. The computation of the half-angle α requires no additional effort as the Green’s functions from all source and receiver points to all subsurface points P have to be computed anyway to determine the isochrone stacking surfaces and weight functions. In this way, the pulse-stretch factor and the reflection coefficient can be determined and made use of implicitly *during* the demigration process (8). Only then, the vertical distance of P to the nearest reflector is stretched locally and the correspondingly computed source pulse is amplified to contribute correctly to the demigration stack.

Approximate solution.—If one would insist on the explicit construction of the artificial migrated section as the first step, the problem of finding the unknown specular reflection angle α_R can still be avoided using one of the following approximations. The first is a small-offset approximation where the reflection coefficients and the stretch factors are replaced by the corresponding quantities for zero offset given by equations (16) and (17). As an alternative, assuming a weak contrast at the reflector, the reflection coefficient can be replaced by a linearized scattering coefficient. If seismic

reflection events with correct first-arrival traveltimes but incorrect pulses are acceptable, the stretch factor can even be omitted. In other words, the reflector images in the artificial migrated section can then be represented in the form

$$M(x, z) = \mathcal{A}(x)F[z - \Sigma(x)] , \quad (18)$$

with \mathcal{A} being some scattering coefficient, e.g., according to the Born approximation. Application of the true-amplitude demigration stack (8) to the reflector image (18) will then result in the seismic reflection response

$$\mathcal{D}(\xi, t) \approx \frac{\mathcal{A}(x^*(\xi))}{\mathcal{L}(\xi)}F[\mathcal{S}(x^*(\xi))^{-1}(t - \mathcal{T}(\xi))] , \quad (19)$$

the traveltimes of which are correct within the validity limits of zero-order ray theory. The amplitudes are, however, correct within the limits of the considered approximation only. In this sense, the seismic forward modeling has been successfully done.

NUMERICAL EXAMPLES

To illustrate the above described method called modeling by demigration, we consider two simple earth models. The first is the one-reflector earth model depicted in Figure 2. The velocities in the half-spaces above and below the reflector were $v_1=2500$ m/s and $v_2=3000$ m/s, respectively. The density was chosen to be constant and equal to unity. For this model, we have simulated a common-offset experiment with a half-offset of $h =500$ m. The ray family for the experiment is also shown in Figure 2. A particular reason for the choice of this model is the presence of a caustic clearly revealed in the figure.

In Figure 3, we see the artificially constructed migrated reflector image obtained from the model parameters. Also indicated are five isochrones for a certain fixed source-receiver pair. Along these and many other isochrones, the amplitudes found in the artificial migrated section are stacked like in a Kirchhoff migration. For each of these stacks, the resulting stack value is placed in the demigrated section into the point determined by the midpoint coordinate of the source-receiver pair and the fixed traveltime defining the isochrone. Note that one of the shown isochrones touches the reflector. It pertains to a primary reflection. The true-amplitude stack along this isochrone will yield the correct amplitude of the corresponding reflection event whereas the stacks along the other isochrones will yield approximately zero. This figure also indicates the Fresnel zone on the reflector, which determines the primary common-offset reflection. The Fresnel zone of a certain

primary reflection is that part of the reflector where its image contributes to the isochrone stack, i.e., where the isochrone cuts the spatial wavelets attached to the reflector (Schleicher et al., 1997).

The common-offset section resulting from modeling by demigration has been compared in Figure 4 with the corresponding sections obtained by conventional seismic modeling schemes. Figure 4a shows the synthetic common-offset seismogram section as obtained by classical zero-order ray theory, and Figure 4b contains the corresponding section resulting from an implementation of the Kirchhoff forward modeling integral (1). Figure 4c shows the new modeling-by-demigration result. Note that in both integration techniques, the aperture was chosen sufficiently large so as to avoid boundary effects. As expected, we observe most fundamental differences between the zero-order ray-synthetic seismograms (Figure 4a) and the ones obtained by both the summation processes. As a main feature, the diffracted events, i.e., the caustic tails in the bow-tie structure are not present in the former. This is due to the well-known fact that standard ray theory does only compute specular reflections and cannot handle nonspecular events. Note that modeling by demigration in this respect is more accurate than zero-order ray theory because it includes diffracted wave branches. This has to be so because, corresponding to Kirchhoff migration, also demigration sums up all possible contributions to a given point in the time section to be constructed. It is hard to see any differences between the Kirchhoff synthetic seismogram section and the one obtained from modeling by demigration.

A closer inspection of the above seismic forward modeling results is provided in Figure 5, where specific single traces are compared. Figure 5a shows the very first trace of the three seismograms of Figure 4 at the midpoint position of 250 m. We clearly see that, for the specular reflection event, modeling by demigration (solid line) yields practically the same pulse as standard zero-order ray theory (dotted line) and Kirchhoff forward modeling (dashed line). The diffracted event that arrives later is quite similar to the one obtained from Kirchhoff modeling. This event is not present in the ray-theoretical seismogram trace. Note, however, that a third, erroneous event is present in the Kirchhoff modeling trace only. It can be explained as a numerical artifact due to insufficient destructive interference of the Kirchhoff summation process. This difficulty is not produced by modeling by demigration, even though the spatial sampling and apertures for both summations were chosen identical. We may say that modeling by demigration at this place is more accurate than Kirchhoff modeling. In Figure 5b, we see the computation results of the three algorithms for the seismic trace at midpoint position 340 m, that is, the fourth trace of Figure 4. For this trace,

the wave propagation involves a caustic. The three methods produce almost identical pulses for the first (specular) reflection, the rays of which pass fairly far away from the caustic. The second (also specularly reflected) event consists of an overlap of two reflections that pass the caustic. The modeling-by-demigration result and the one from Kirchhoff modeling do not show significant differences. The amplitudes of the caustic events differ slightly, but we do not have a criterion on which one is a better approximation of the correct amplitude. Note the wrongly large amplitudes provided by ray theory for this caustic situation. This is due to the known phenomenon that ray theory overestimates amplitudes when the receiver is too close to a caustic. Figure 5c depicts the results of the three methods for the construction of the trace at 430 m, i.e., the seventh trace of Figure 4. This trace is interesting because it is exactly in the center of the bow tie structure, where there is an overlap between all three specularly reflected pulses. Of the three corresponding reflected rays, two of them pass through the caustic point, the third one does not. Ray amplitudes should be correct here, because the receiver position is sufficiently far away from the caustic location. We see that modeling by demigration in this case seems to give a better result than Kirchhoff modeling. The pulse obtained by modeling by demigration fits the ray traced pulse quite well but there is a certain amplitude loss in the Kirchhoff result. Figure 5d confirms this observation. It depicts the seismic trace from the very left of the model, i.e., with a midpoint coordinate of 850 m, where there is no influence of the caustic. Again, ray theory should give an exact result. We see that the pulse obtained from modeling by demigration fits again the ray-theoretical pulse very well in amplitude and pulse shape. The amplitude obtained by Kirchhoff modeling is also more or less the same. However, whereas the pulse form of modeling by demigration and ray theory are practically identical, we see that the Kirchhoff modeling counterpart pulse has suffered some distortion. It is longer than the original source wavelet, and its second leg is less deep than the correct one.

As a final comparison for this model, we address in Figure 6 the amplitudes along the whole seismic sections obtained from the three different methods. We have picked the peak amplitudes of the two distinguishable events in the three sections. Note that for the amplitudes of the first event (see Figure 6a), modeling by demigration (solid line) reconstructs the same amplitude values as ray theory (dotted line) until a midpoint coordinate of about 400 m. Kirchhoff modeling (dashed line), however, suffers from a certain amplitude loss. Between about 400 m and 500 m, ray tracing suffers from incorrect amplitudes because the receiver falls into the near vicinity of the caustic point and the two arrivals overlap. Here, we see that the amplitudes of modeling by demigration follow more closely the ones obtained from Kirchhoff modeling. Beyond 500 m, all three approximations yield

comparable results. Observe that Kirchhoff modeling systematically yields the lowest amplitudes. From the amplitudes of the second event (see Figure 6b), we may again observe that modeling by demigration and Kirchhoff modeling provide quite similar results for the diffracted events and the ones close to the caustic. As already indicated, ray theory yields wrong amplitudes in this region. Again, Kirchhoff modeling seems to slightly underestimate the amplitudes.

One might argue that the slightly lower amplitudes of Kirchhoff modeling in comparison to modeling by demigration can be reduced with a smaller sampling interval in the numerical integration. However, it should be kept in mind that in the present example, both integrals were numerically solved using the same sampling interval as well as the same numerical integration technique and are thus directly comparable.

To demonstrate another advantage of modeling by demigration over the conventional modeling schemes, we have chosen the second example. The velocities were chosen as before, and the reflector is now a nonsmooth interface consisting of linear segments (see Figure 7). This is typical in practical situations in which the reflectors have to be picked from a migrated seismic image. Figure 8 shows the three modeling results as obtained from zero-order ray theory (Figure 8a), Kirchhoff modeling (Figure 8b), and modeling by demigration (Figure 8c). We see conflicting dips in the seismograms and a shadow zone where no specularly reflected ray is observed (see also the ray family in Figure 7). Correspondingly, the ray-theoretic section (Figure 8a) suffers from a gap in the reflected event. Kirchhoff modeling (Figure 8b) accounts for wavefront healing effects, but produces a lot of spurious events. This is due to the problems with the nonsmoothness of the interface and the ill-defined surface normal needed in the Kirchhoff integral. Only the modeling-by-demigration scheme (Figure 8c) shows a nice wavefront healing without producing additional, nonphysical events. It smoothes over the edge points of the reflector, thus resulting in the physically most reasonable synthetic data section of the three computed ones.

SUMMARY AND CONCLUSIONS

We have proposed a new seismic forward modeling scheme that is based on a seismic imaging process called demigration. The latter process has been introduced in the seismic literature as the most natural inverse process to migration. For a given subsurface model, the newly proposed seismic modeling process conceptually consists of two steps. These are (i) the transformation of the

given subsurface model into a fictitious, artificial true-amplitude depth-migrated section and (ii) the application of a true-amplitude demigration to this artificially constructed migrated section. The construction of the artificial migrated section can be done implicitly so that modeling by demigration is, in fact, a one-step process.

For a single reflector situation where a caustic point is present, and for a nonsmooth reflector consisting of linear segments, we have compared the results obtained by the proposed scheme with their counterparts obtained from conventional classical ray-theoretical and Kirchhoff forward modeling. For these simple but typical examples that include diffractions, conflicting dips and even a caustic, modeling by demigration has provided superior results than the conventional processes of Kirchhoff modeling and zero-order ray theory.

In particular, in regions where ray theory is expected to yield good results, modeling by demigration has provided specular reflection pulses that are almost identical to those of ray theory, i.e., they have suffered very little from pulse stretch, phase shifts, or amplitude losses. At the same time, it has accounted for diffractions in a very similar way as conventional Kirchhoff modeling. Thus, we may conclude that modeling by demigration combines the advantages of both conventional methods.

Another advantage of modeling by demigration over both other methods is its little sensitivity to nonsmooth reflectors. Even in situations where synthetic data computed by zero-order ray theory or the Kirchhoff forward modeling integral are severely affected by the nonsmoothness of a reflector, modeling by demigration turned out to work reasonably well.

As a final remark, it is to be observed that modeling by demigration is especially well suited to perform modeling in time-lapse applications, i.e., to model reservoir changes with time. As in this case only the artificial migrated section has to be changed, the previously computed stacking surfaces and weight functions can be used again without any modifications.

ACKNOWLEDGMENTS

We are grateful to Norman Bleistein and Herman Jaramillo for fruitful discussions with respect to the subject. The present research has been financed in part by the Brazilian National Research Council (CNPq), the State Research Foundation of São Paulo (FAPESP), the German Academic Exchange Service (DAAD), and the sponsors of the WIT consortium at Karlsruhe University. This is Karlsruhe University, Geophysical Institute Publication Number 837.

REFERENCES

- Bleistein, N., 1987, On the imaging of reflectors in the earth: *Geophysics*, **52**, 931–942.
- Brown, R., 1994, Image quality depends on your point of view: *The Leading Edge*, **13**, 669–673.
- Fagin, S.W., 1994, Demigration – a better way to derive an interpretation of unmigrated reflections: Summer workshop, EAEG/SEG, Expanded Abstracts, 38–39.
- Faye, J.P., and Jeannot, J.P., 1986, Prestack migration velocities from focusing depth analysis: 56th Ann. Internat. Mtg., Soc. Expl. Geophys., Expanded Abstracts, 438–440.
- Ferber, R.G., 1994, Migration to multiple offsets and velocity analysis: *Geophys. Prosp.*, **42**, 99–112.
- Frazer, L.N., and Sen, M.K., 1985, Kirchhoff-Helmholtz reflection seismograms in a laterally inhomogeneous multi-layered elastic medium – I. Theory: *Geophys. J. Roy. Astr. Soc.*, **80**, 121–147.
- Hubral, P., Schleicher, J., and Tygel, M., 1996, A unified approach to 3-D seismic reflection imaging – Part I: Basic concepts: *Geophysics*, **61**, 742–758.
- Jaramillo, H., and Bleistein, N., 1997, Demigration and migration in isotropic inhomogeneous media: 67th Ann. Internat. Mtg., Soc. Expl. Geophys., Expanded Abstracts, 1673–1676.
- Kaculini, S., 1994, Time migration and demigration in 3D: Summer workshop, EAEG/SEG, Expanded Abstracts, 66–69.
- Lailly, P., and Sinoquet, D., 1996, Smooth velocity models in reflection tomography for imaging complex geological structures: *Geophys. J. Internat.*, **124**, 349–362.
- Schleicher, J., Hubral, P., Tygel, M., and Jaya, M.S., 1997, Minimum apertures and Fresnel zones in migration and demigration: *Geophysics*, **62**, 183–194.
- Schleicher, J., Tygel, M., and Hubral, P., 1993, 3-D true-amplitude finite-offset migration: *Geophysics*, **58**, 1112–1126.
- Sheriff, R.E., 1975, Factors affecting seismic amplitudes: *Geophys. Prosp.*, **23**, 125–138.
- Sun, J., and Gajewski, D., 1997, True-amplitude common-shot migration revisited: *Geophysics*, **62**, 1250–1259.

- Tygel, M., Schleicher, J., and Hubral, P., 1994a, Kirchhoff-Helmholtz theory in modelling and migration: *J. Seis. Expl.*, **3**, 203–214.
- Tygel, M., Schleicher, J., and Hubral, P., 1994b, Pulse distortion in depth migration: *Geophysics*, **59**, 1561–1569.
- Tygel, M., Schleicher, J., and Hubral, P., 1995, Dualities between reflectors and reflection-time surfaces: *J. Seis. Expl.*, **4**, 123–150.
- Tygel, M., Schleicher, J., and Hubral, P., 1996, A unified approach to 3-D seismic reflection imaging – Part II: Theory: *Geophysics*, **61**, 759–775.
- Whitcombe, D.N., 1991, Fast and accurate model building using demigration and single-step ray-trace migration: *61st Ann. Internat. Mtg., Soc. Expl. Geophys., Expanded Abstracts*, 1175–1178.
- Whitcombe, D.N., 1994, Fast model building using demigration and single-step ray migration: *Geophysics*, **59**, 439–449.

GLOSSARY

S	Source position
G	Receiver position
ξ	Coordinate of the source-receiver pair (S, G) (2-D vector) in the original time section
ξ^*	Stationary point of the Kirchhoff migration integral
t	time coordinate
\mathbf{x}	Horizontal coordinate (2-D vector)
\mathbf{x}^*	Stationary point of both Kirchhoff modeling and Kirchhoff demigration integrals
z	Depth coordinate
P	Point with coordinates (\mathbf{x}, z) in depth
P_Σ	Point on the reflector with coordinates $(\mathbf{x}, \Sigma(\mathbf{x}))$
P_R	Stationary point on the reflector with coordinates $(\mathbf{x}^*, \Sigma(\mathbf{x}^*))$
Σ	Reflector surface defined as $z = \Sigma(\mathbf{x})$
ζ	Isochron surface defined as $z = \zeta(\mathbf{x}, \xi, t)$
T	Traveltime between two points
$\tau(\xi, P_\Sigma)$	Traveltime from $S(\xi)$ to P_Σ to $G(\xi)$
$\mathcal{T}(\xi)$	Reflection traveltime from $S(\xi)$ to P_R to $G(\xi)$
$F[t]$	Analytic source pulse
$D(\xi, t)$	Time-domain data
$M(\mathbf{x}, z)$	Migrated data
$\mathcal{K}(\xi, t)$	Kirchhoff synthetic section
$\mathcal{M}(\mathbf{x}, z)$	Kirchhoff migrated section
$\mathcal{D}(\xi, t)$	Kirchhoff demigrated section
$W(\xi, P_\Sigma)$	Weight function for the Kirchhoff modeling integral
$W_M(\xi, P)$	Weight function for the Kirchhoff migration integral
$W_D(\mathbf{x}, \xi, t)$	Weight function for the Kirchhoff demigration integral

\mathcal{R}	angle-dependent reflection coefficient at the target reflector	
\mathcal{L}	3-D geometrical-spreading factor of the reflection ray from S to G	
\mathcal{S}	Migration stretch factor	
\mathcal{P}	Prestretch factor for modeling by demigration	
\mathcal{A}	Amplitude factor for modeling by demigration	\ae
α_R	Reflection angle at P_R	
β_R	Local in-plane reflector dip angle at P_R	
ρ_R^\pm	Density at P_R above/below the reflector	
v_R^\pm	Acoustic wave velocity at P_R above/below the reflector	

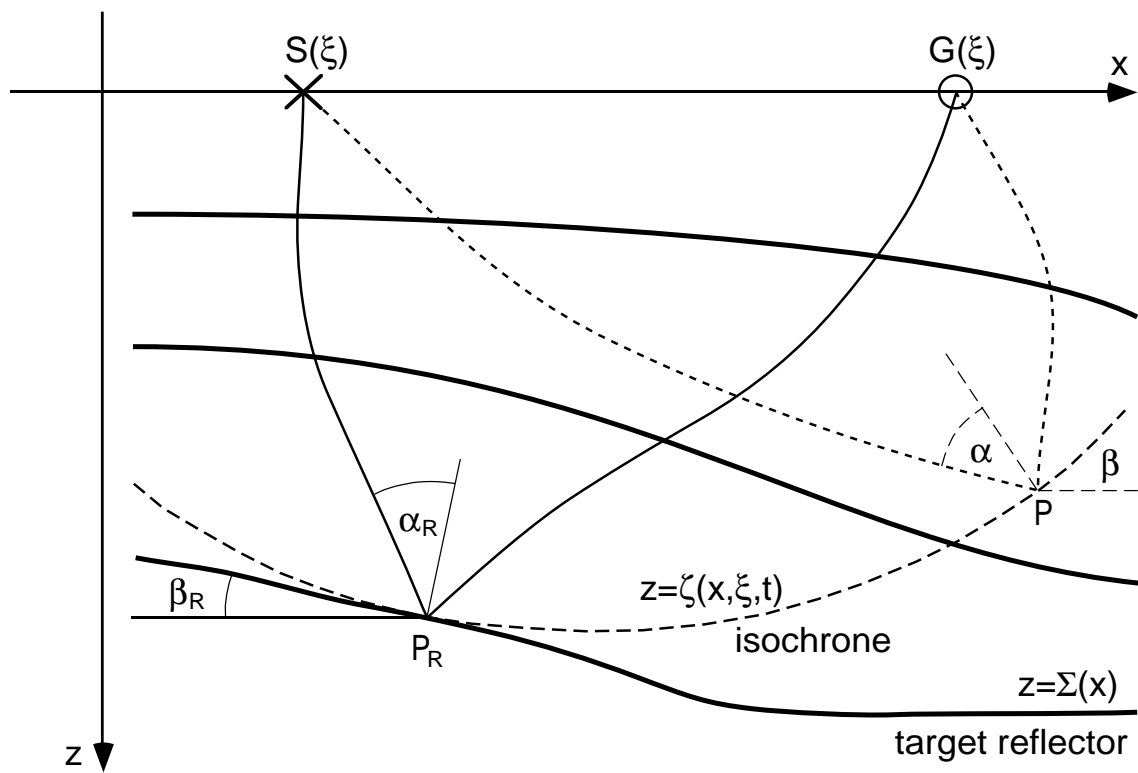


FIG. 1: Inhomogeneous earth model with smooth interfaces. Also shown is one isochrone for the indicated source-receiver pair.

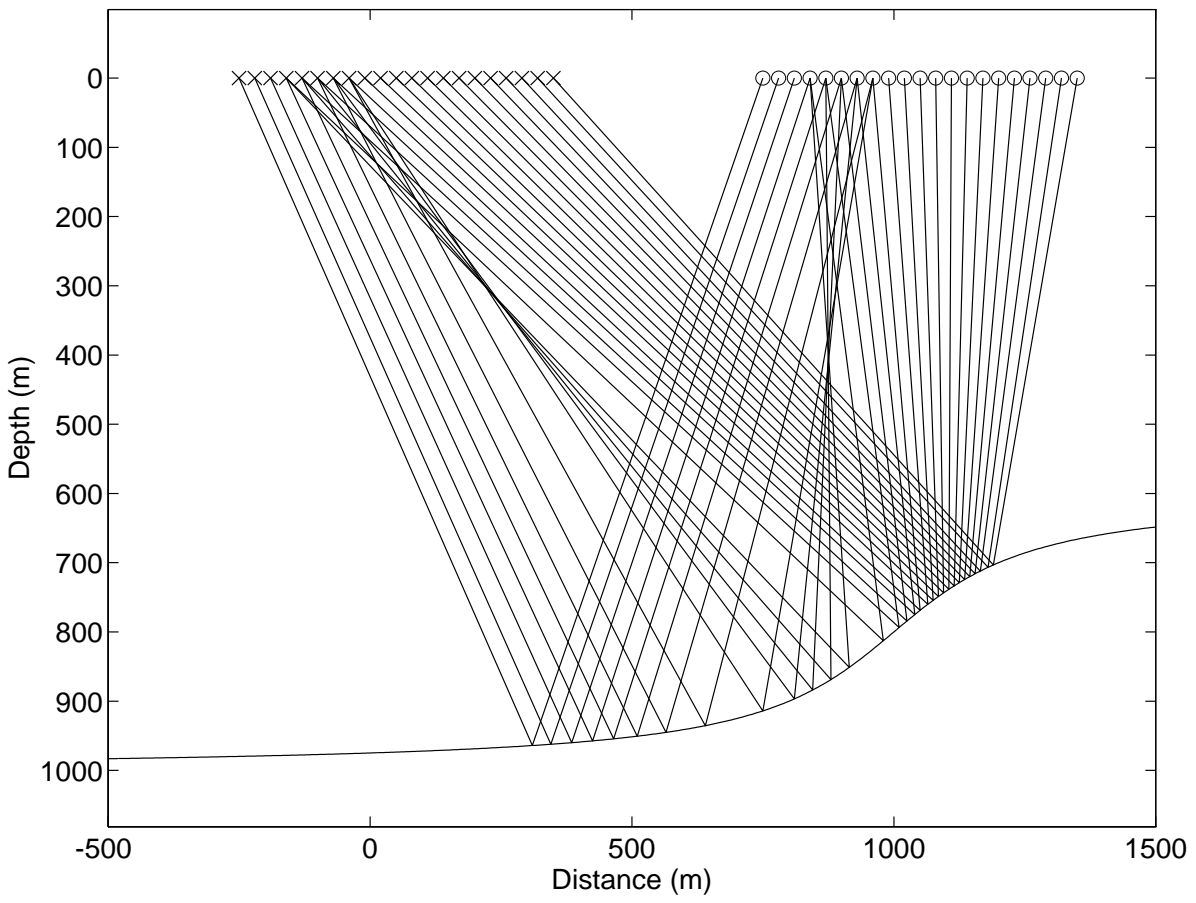


FIG. 2: One-layer model for the numerical experiment.

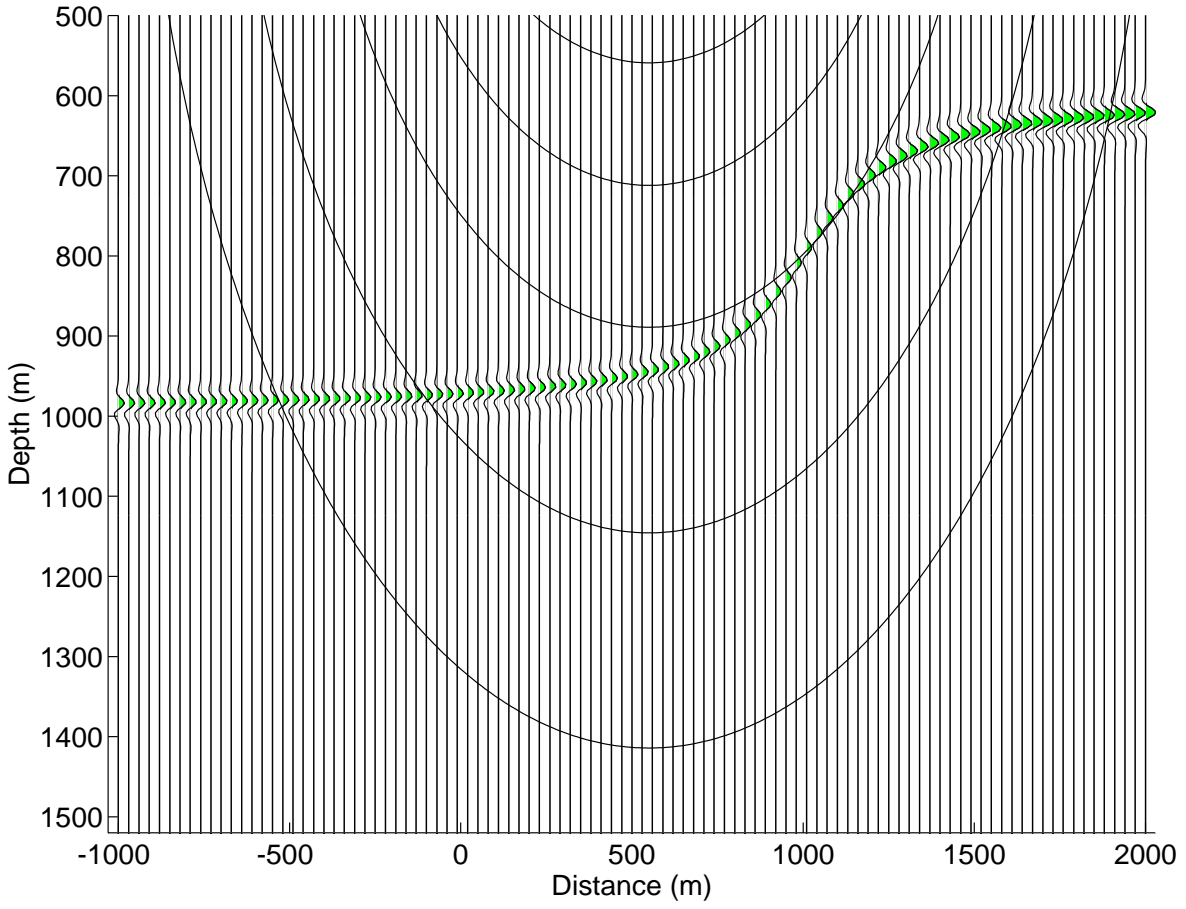


FIG. 3: Artificial migrated section constructed from the model parameters shown in Figure 2.

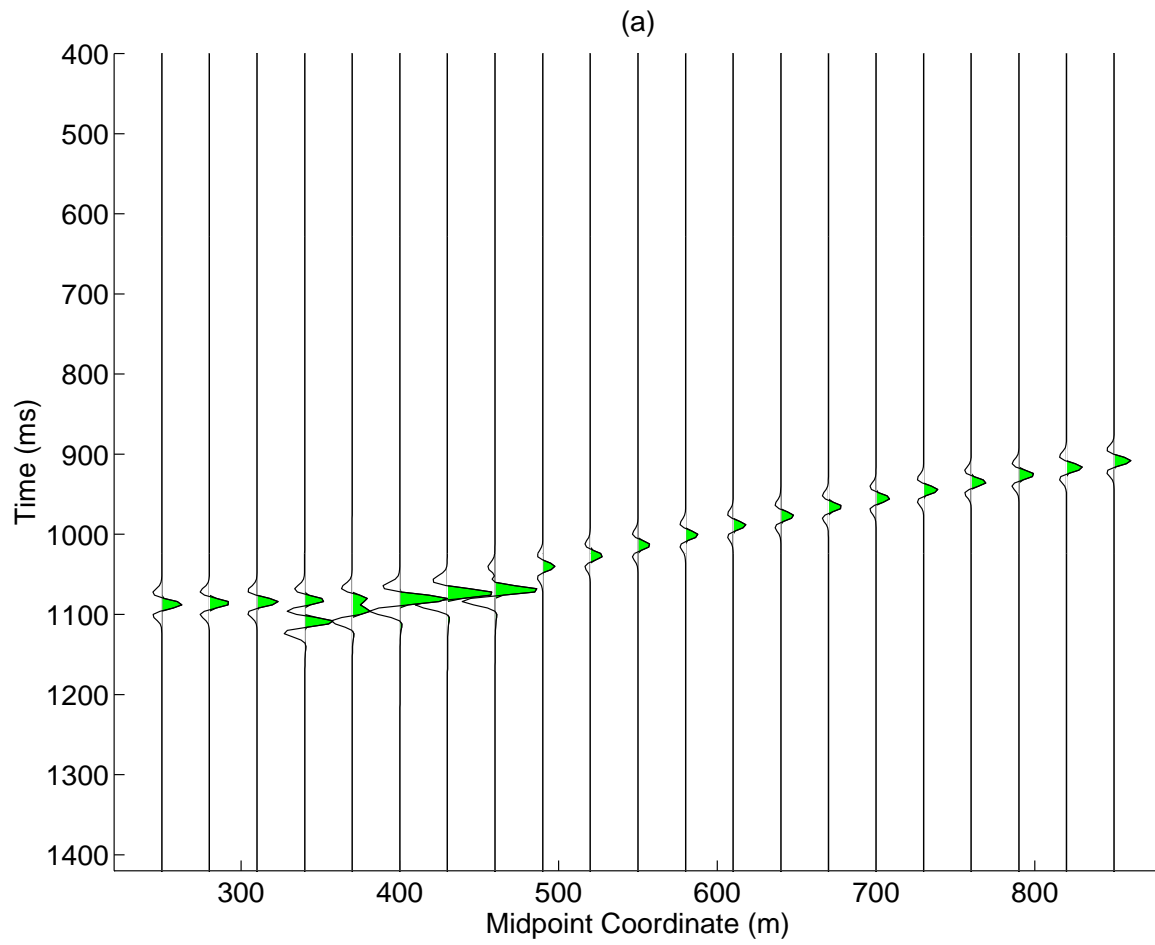


FIG. 4A: Modeled common-offset section as a result of zero-order ray theory.

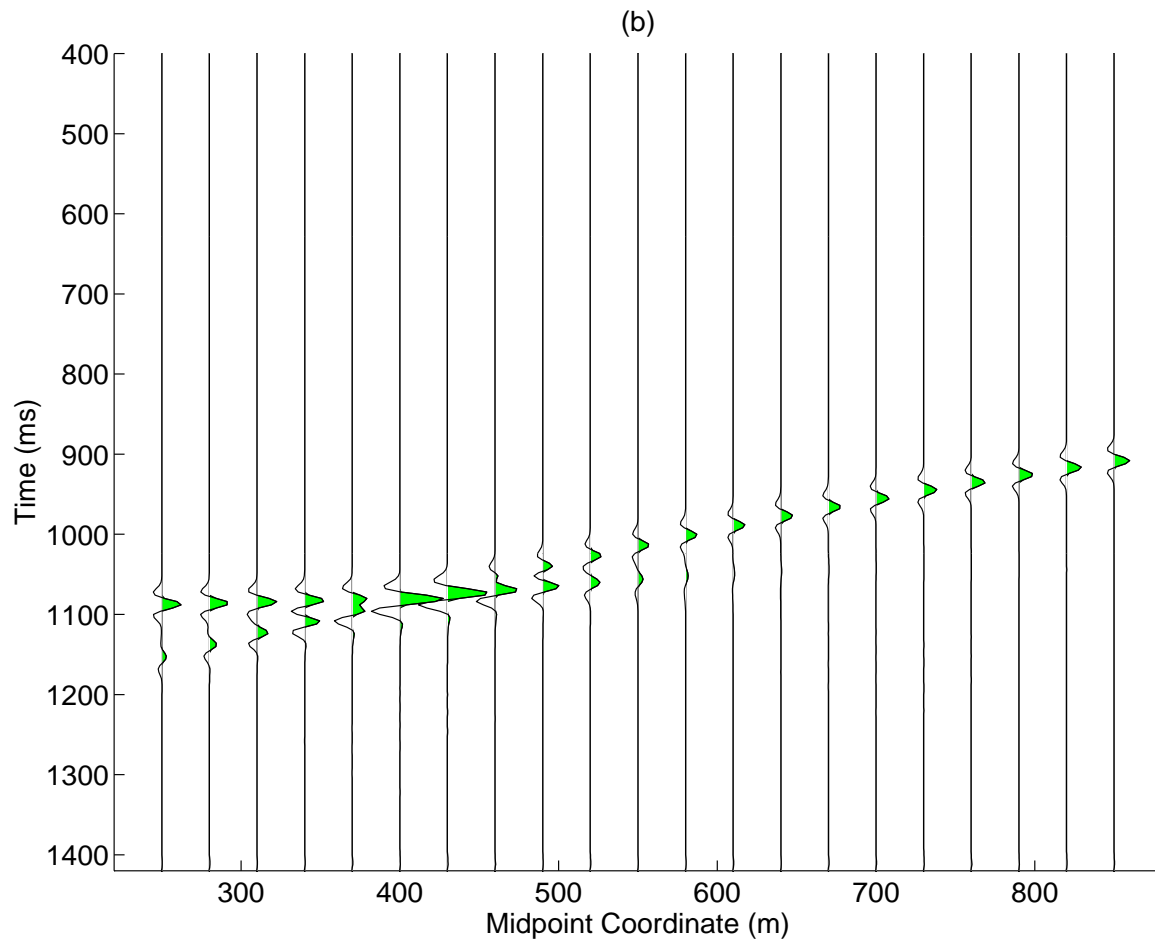


FIG. 4B: Modeled common-offset section as a result of the Kirchhoff integral.

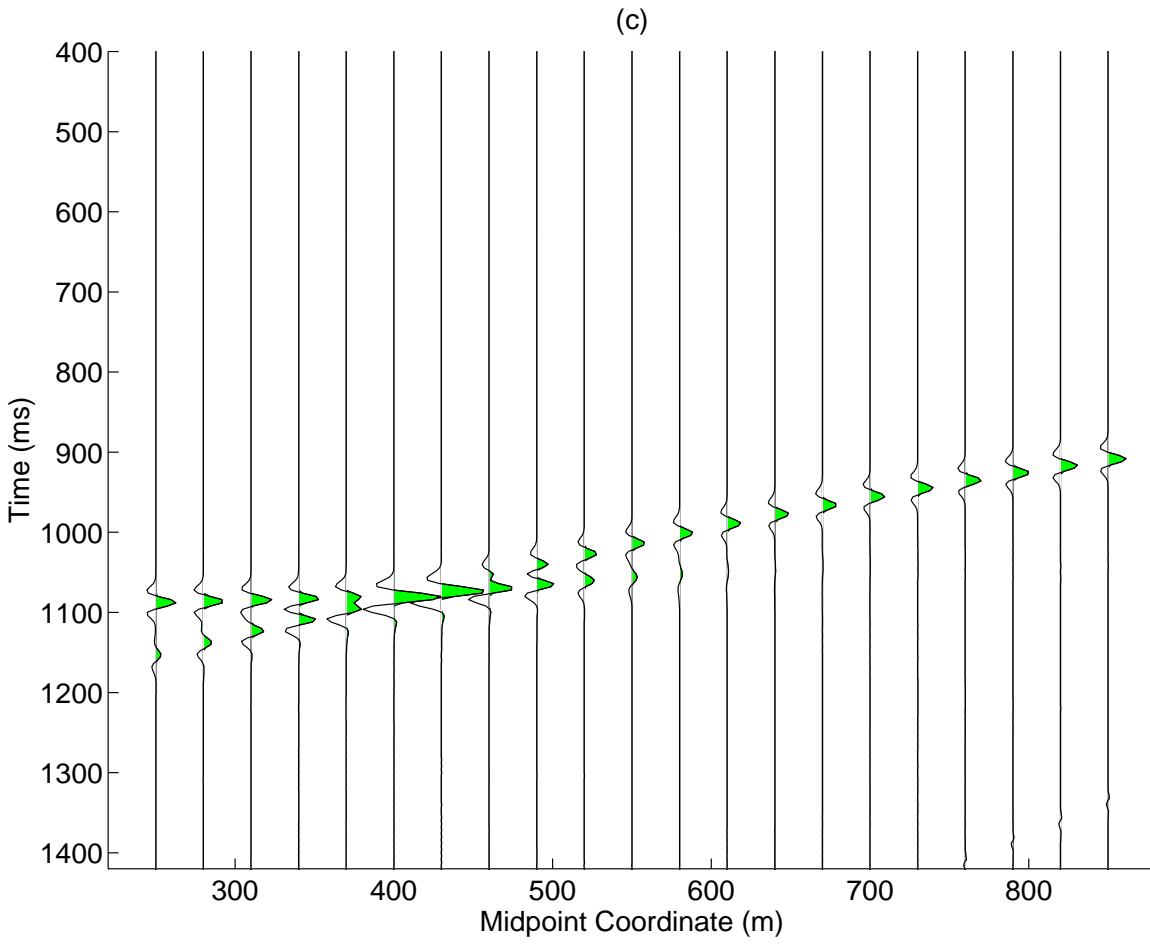


FIG. 4C: Modeled common-offset section as a result of modeling by demigration.

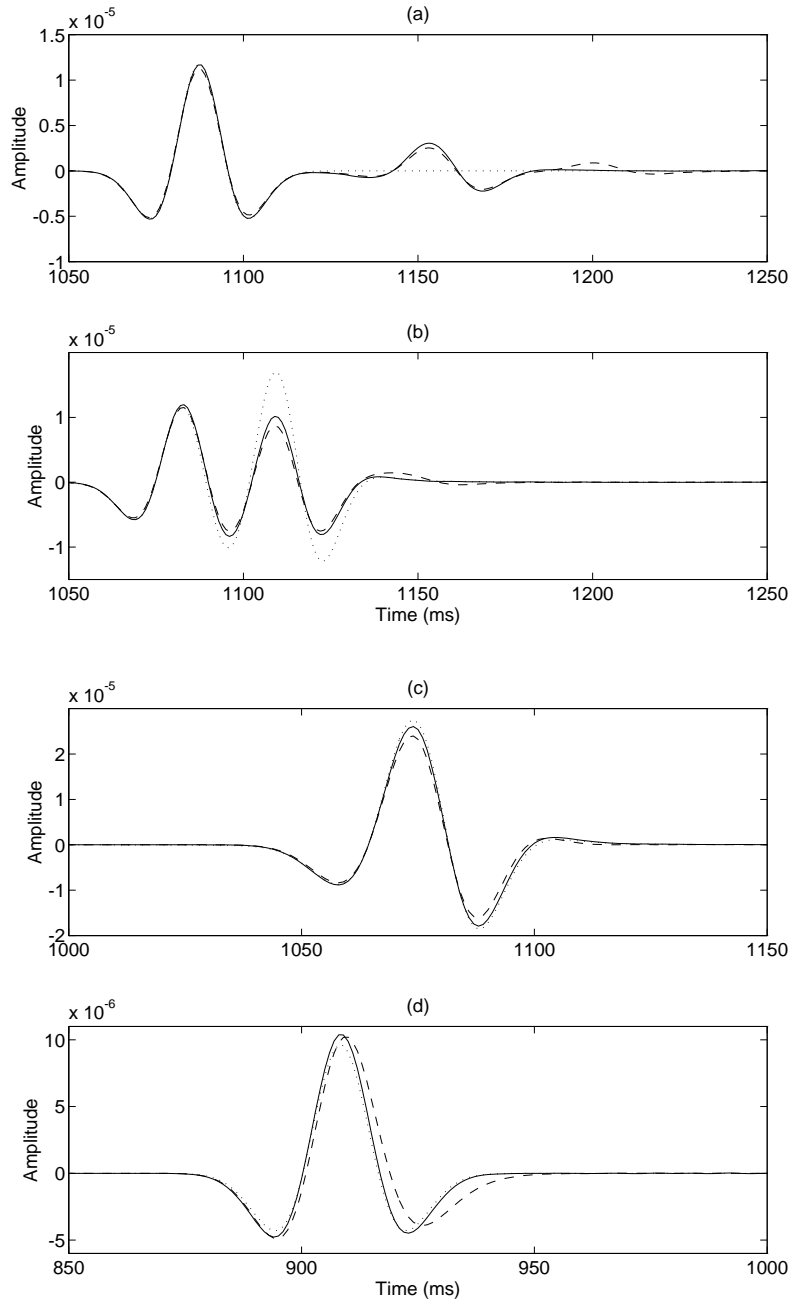


FIG. 5: Comparison of the modeling results of zero-order ray theory (dotted line), Kirchhoff modeling (dashed line), and modeling by demigration (solid line). (a) Trace at midpoint 250 m. (b) Trace at midpoint 340 m. (c) Trace at midpoint 430 m. (d) Trace at midpoint 850 m.

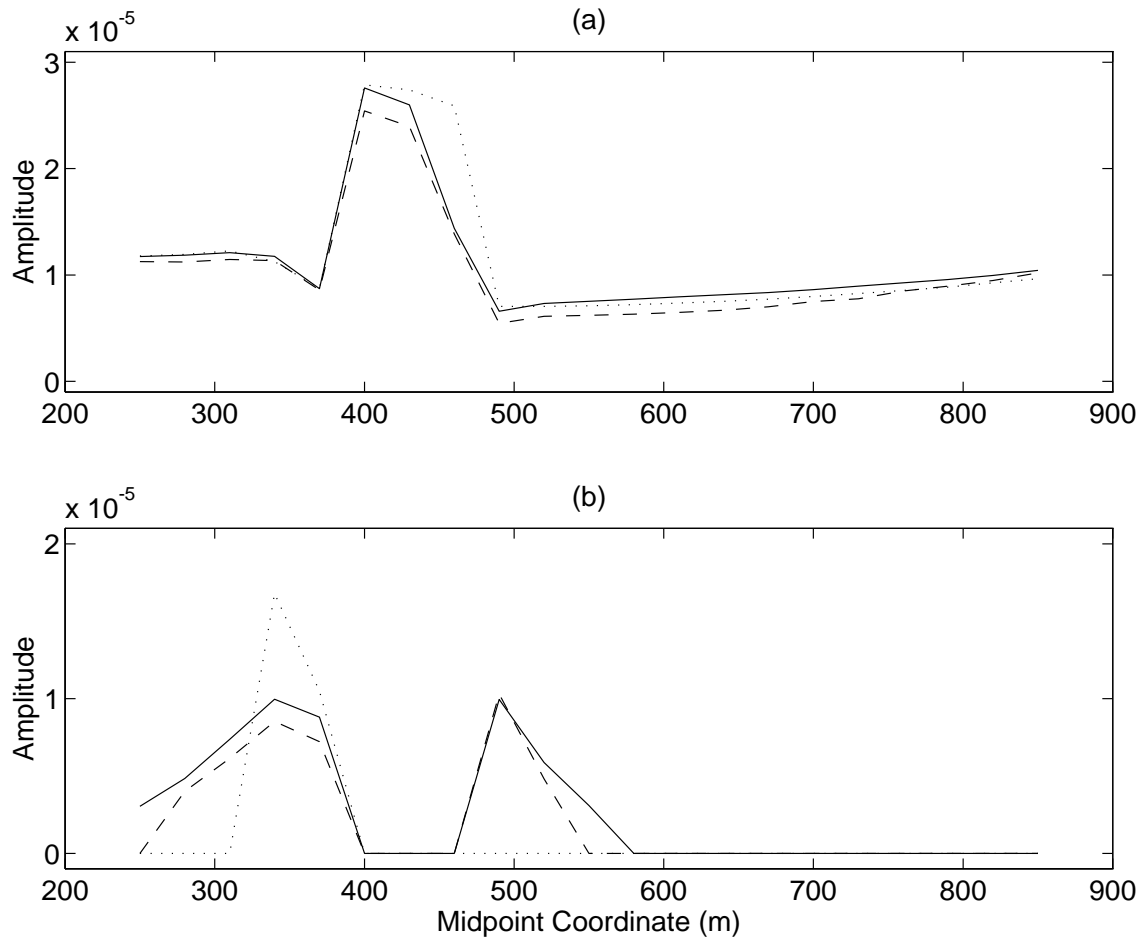


FIG. 6: Comparison of the amplitude values along the reflections in Figure 4 as obtained from zero-order ray theory (dotted line), Kirchhoff modeling (dashed line), and modeling by demigration (solid line). (a) First arrival. (b) Second arrival.